

New carbon nitride phase by high-dose N ion implantation in glassy carbon

S. P. Withrow, J. M. Williams, S. Praver, and D. Barbara

Citation: [Journal of Applied Physics](#) **78**, 3060 (1995); doi: 10.1063/1.360057

View online: <http://dx.doi.org/10.1063/1.360057>

View Table of Contents: <http://scitation.aip.org/content/aip/journal/jap/78/5?ver=pdfcov>

Published by the [AIP Publishing](#)

Articles you may be interested in

[Formation of nanovoids in high-dose hydrogen implanted GaN](#)

Appl. Phys. Lett. **89**, 031912 (2006); 10.1063/1.2221526

[Depth analysis of phase formation in \$\alpha\$ -Fe after high-dose Al ion implantation](#)

J. Appl. Phys. **84**, 6570 (1998); 10.1063/1.369030

[Spectroscopic characterization of phases formed by high-dose carbon ion implantation in silicon](#)

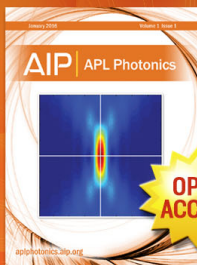
J. Appl. Phys. **77**, 2978 (1995); 10.1063/1.358714

[Formation of ferromagnetic iron nitrides in iron thin films by high-dose nitrogen ion implantation](#)

J. Appl. Phys. **65**, 4357 (1989); 10.1063/1.343272

[Formation of silicon nitride compound layers by high-dose nitrogen implantation](#)

J. Appl. Phys. **51**, 1605 (1980); 10.1063/1.327763



Launching in 2016!

The future of applied photonics research is here

OPEN
ACCESS

AIP | APL
Photonics

New carbon nitride phase by high-dose N ion implantation in glassy carbon

S. P. Withrow and J. M. Williams

Oak Ridge National Laboratory, Oak Ridge, Tennessee 37831

S. Praver and D. Barbara

School of Physics, University of Melbourne, Parkville, Victoria 3052, Australia

(Received 2 March 1995; accepted for publication 18 May 1995)

The possibility for the synthesis of CN compounds by high-dose N implantation of glassy carbon is investigated. The changes in volume and surface morphology and the retained N concentration as a function of ion dose are reported. For both N and C (used as a control), implantation initially induces compaction in the surface region that saturates at a density above 2.6 g/cm^3 . After formation of this dense surface layer, additional implantation causes the material to expand to accommodate the implanted ions and vacancies formed during the implantation process. For N the swelling is initially linear in fluence up to $5 \times 10^{17} \text{ /cm}^2$ with a volume increase of 16 \AA^3 per added N atom; this is twice the volume per atom in the compacted substrate. Above a dose of $5 \times 10^{17} \text{ N/cm}^2$ the swelling behavior is more complex. A phase change is observed to occur at a dose between 5×10^{17} and $1 \times 10^{18} \text{ /cm}^2$, which is concomitant with at least some of the implanted N being driven to the surface. In addition, micron-sized surface features are seen by scanning electron microscopy, and a significant surface roughening occurs. Ion backscattering spectra have been used to characterize the implanted N profile. The maximum retained concentration was found to be 30 at. %. © 1995 American Institute of Physics.

INTRODUCTION

Over the past few years there has been interest in growing a solid formed from C and N and having the same structure as $\beta\text{-Si}_3\text{N}_4$. Theoretical predictions suggest that such a phase could be metastable and would have interesting properties, including hardness, thermal, and electronic properties that are comparable to diamond.¹ A variety of techniques have been employed to produce this material, including film formation using ion-beam deposition,²⁻⁸ ion implantation,⁹⁻¹⁴ plasma deposition,¹⁵⁻¹⁷ pyrolysis,^{18,19} and shock wave compression.²⁰ While some interesting C-N structures have been synthesized, only limited success has been reported in achieving a N content approaching the 57 at. % needed for C_3N_4 .

The present work is part of an effort to produce C-N phases by introducing nitrogen into glassy carbon (GC) using ion implantation. The ability of the ion implantation technique to modify materials far from equilibrium conditions makes it ideal for metastable materials synthesis. Implantation is a versatile technique, allowing some control over stoichiometry through the amount and depth of implanted material.

Several groups have reported results from ion implantation into GC. Iwaki, Takahashi, and Sekiguchi²¹ investigated the properties of GC implanted with N to doses between 5×10^{14} and $5 \times 10^{16} \text{ /cm}^2$. The wear properties of the irradiated material improved with increasing dose and decreasing implantation temperature. However, as has been made clear in many other studies (e.g., McCulloch, Praver, and Hoffman,²² and references therein) the increase in wear resistance is damage driven and is not due to chemical effects (at least for the dose range used in those experiments). At a dose of about 0.5 displacement per atom (dpa), a compacted,

amorphous surface layer is formed containing about 15% sp^3 -type bonds, and it is the formation of this layer that accounts for the increase in wear resistance.

Subsequent studies by McCulloch and Praver²³ have shown that both interstitials and vacancies are immobile in GC for implantations performed well below room temperature. The dynamic annealing which accompanies elevated temperature implantations inhibits the formation of the aforementioned dense amorphous layer, and this is the reason why the wear resistance decreases with increasing implantation temperature.

Attempts to produce CN phases by low-energy (250–1000 eV) ion implantation of highly oriented pyrolytic graphite have recently been reported.¹¹ Three different C-N bonding states were reported, one of which was consistent with the sought-after $\beta\text{-C}_3\text{N}_4$ phase; however, the C-N stoichiometry in such systems is largely sputter limited. Recent work by Hoffman *et al.* using 25–50 keV N implantation of GC has reported a maximum N concentration of between 25 and 30 at. % for high-dose (10^{18} N/cm^2) implants.^{12,13} A similar N concentration was observed by McCulloch;¹⁴ however, for the 50 keV energies used, the shape of the N peak in the Rutherford backscattering (RBS) spectrum suggested that the N concentration may have been sputter limited.

The focus of the present work is to gain an understanding of those factors which control the N stoichiometry in high-dose N-implanted GC. For this purpose, low-temperature implantations were performed in order to limit N mobility during the implantation. In addition, N implantations were performed at higher energies (160 keV) than previously employed so as to put the N deeper into the sample

and thus decrease the effects of sputtering in limiting the maximum N concentration achievable.

EXPERIMENTAL PROCEDURES

The glassy carbon (V25 grade) used in this study was heat treated to 2500 °C and has a density of 1.55 g/cm³. It was purchased in plate form²⁴ and cut into 2×1×0.25 cm³ experimental samples. The implantation surface was polished to a mirror finish using 1 μm diamond paste on a cloth lap. Polishing cleans the surface of impurities and assures that the starting surface condition for all implants is the same. Samples were implanted with N ions at 160 keV or C ions at 135 keV at selected doses up to 2×10¹⁸/cm². The implantation energies were chosen using the PROFILE code²⁵ to put the peak of the distribution for both species at the same depth. For virgin material the depth is ~410 nm. As shown below, the density of the material, and hence the depth of implant, changes with dose. The samples were held at -100 °C during implantation. As mentioned above, at this temperature both vacancies and interstitials are immobile so that extended defects are not expected to be formed during the implantation and the N mobility is expected to be small. A constant dose rate of 6.2 μA/cm² was used. Part of the surface was masked to preserve an unimplanted region. A profilometer²⁶ was used to measure the step height between the implanted and unimplanted regions as a function of dose. Surface roughness changes were also determined using the same instrument. Rutherford backscattering spectra were obtained using 2 MeV ⁴He⁺ to characterize the distribution of the implanted N. Selected samples have also been examined using a scanning electron microscope (SEM).

RESULTS

The height of the step on the surface between implanted and unimplanted regions is shown in Fig. 1 as a function of dose. Results are shown for both N and C implantation. GC behaves qualitatively the same for both ion species. Below 1×10¹⁵/cm² a step is not resolvable from the surface roughness. Above 1×10¹⁵/cm² compaction of the implanted layer, graphed as a negative step height in Fig. 1, is initially observed up to a dose where a maximum negative step height of 190 nm is measured. In the case of N implantation the densification saturates at a dose of 3×10¹⁶/cm², corresponding to a dpa of 3 at the peak of the implantation distribution.²⁷ Nearly the same size step is observed for the lighter and less energetic C at a somewhat higher dose. At maximum compaction for N implantation the N ions make up less than 1% of the atomic species in the compacted layer. A rough estimate of the effect of sputtering of the sample was obtained by preimplanting a low-dose Ar marker and measuring the change in depth of the marker with N implantation using RBS. The results indicated the sputter yield was ≤1. The sputter yield for N bombardment of C at 160 keV has been reported to be 0.1–0.2.²⁸

With additional implantation the GC expands in the normal direction. No saturation in expansion is measured up to the highest doses used. For a sufficient dose, the profilometer measures a step up from the unimplanted to the implanted

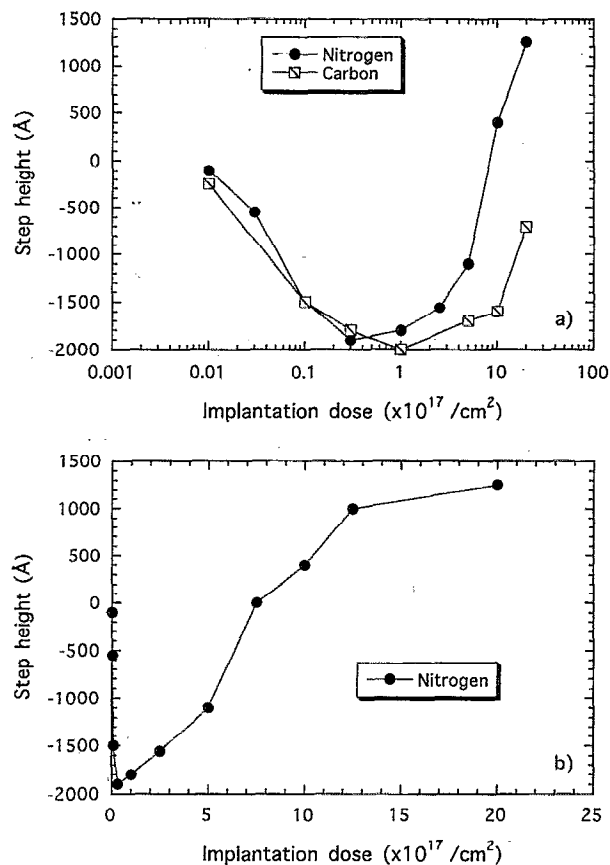


FIG. 1. (a) Measured step height between unimplanted and implanted areas on glassy carbon surface as a result of 160 keV N (solid circles) and 135 keV C (squares) implantation at -100 °C. Negative step height indicates contraction of implanted region. (b) Step height for N implantation plotted on a linear dose scale.

region. In Fig. 1(b) the expansion region for N implantation is plotted on a linear scale. Between 0.3 and 5×10¹⁷ cm² the expansion is linear with implantation dose. Above 5×10¹⁷/cm² the expansion versus dose curve is no longer linear, indicating that something more complex is occurring to accommodate the implanted ions. We suggest below that there may be a phase change occurring at about this dose.

The surface roughness on both implanted and unimplanted samples was also determined using the step height profilometer. The measurements were calculated by scanning across 200 μm of the surface, determining a mean line through the trace, and calculating an average deviation from the mean.²⁶ Results are shown in Fig. 2. The dashed line in this figure shows the surface roughness of unimplanted GC. Samples implanted with carbon show no significant change in roughness from the unimplanted results up to the highest doses used. A similar result is also obtained for nitrogen implantation up to a dose of 1×10¹⁷/cm². Above this dose, however, the surface roughness for N-implanted samples increases dramatically, with a change of more than an order of magnitude measured at a dose of 2×10¹⁸ N/cm². The surface roughening was also observed visually as a change in color from shiny black to a flat gray appearance.

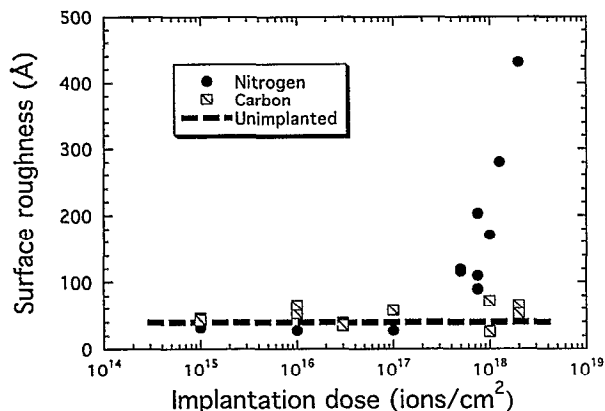


FIG. 2. Surface roughness following implantation of N (160 keV) or C (135 keV) into glassy carbon.

The surfaces of implanted samples have also been observed using a SEM. For implantation at 1×10^{17} N/cm² no surface features other than polishing scratches left from sample preparation are seen although the implanted region appears darker. Micrographs taken from samples implanted at 5 – 20×10^{17} N/cm² are given in Figs. 3(a)–3(c). The unimplanted surface is visible at the left-hand side of each of these figures. At the lowest dose shown, ion bombardment causes an overall darker surface in the SEM and the appearance of linear features, the most prominent of which follow polishing scratches. At 1×10^{18} N/cm², however, these lines have been replaced by an interwoven pattern of irregular, elongated “ribbon” or “wormlike” features with dimensions less than a micron across and several microns in length; these features appear to emerge from the surface and completely cover the implanted region. By a dose of 2×10^{18} N/cm² the surface structure is more rounded and higher, consistent with the enhancement in roughness seen in Fig. 2. A micrograph from GC implanted with C to 2×10^{18} /cm² is given in Fig. 3(b). A patterned surface topography is observed which is not unlike that seen at a dose of 5×10^{17} for N implantation. No implant-induced structure is seen for lower C doses.

Rutherford backscattering spectra from GC implanted with N at 1.0 – 5.0×10^{17} /cm² are presented in Fig. 4(a) and for higher doses in Fig. 4(b). A virgin spectrum from an unimplanted GC sample is given as a dashed line in Fig. 4(a) for comparison. Changes from the virgin spectrum are seen with implantation. The accumulation of N at the end of the implant range is observed as an increase in the yield between roughly 0.42 – 0.52 MeV over the yield in the virgin spectrum. In addition, the decrease in signal between about 0.25 and 0.42 MeV (the deficit) results from a decrease in the local carbon atomic percent in the implanted layer. With increasing N dose, the N atomic percent at the end of range increases and the C atomic percent decreases. The arrow in Fig. 4(a) indicates the energy for He scattering from N at the surface. For implantation up to 5×10^{17} , the N remains localized at its implant range. The small yield just above 0.7 MeV is due to oxygen at the surface. As can be seen in Fig. 4(b), the implanted N becomes mobile at higher fluences. For a dose of 1×10^{18} /cm² N has moved to the surface. At 2×10^{18} /cm² there is yet more N at the surface and the N

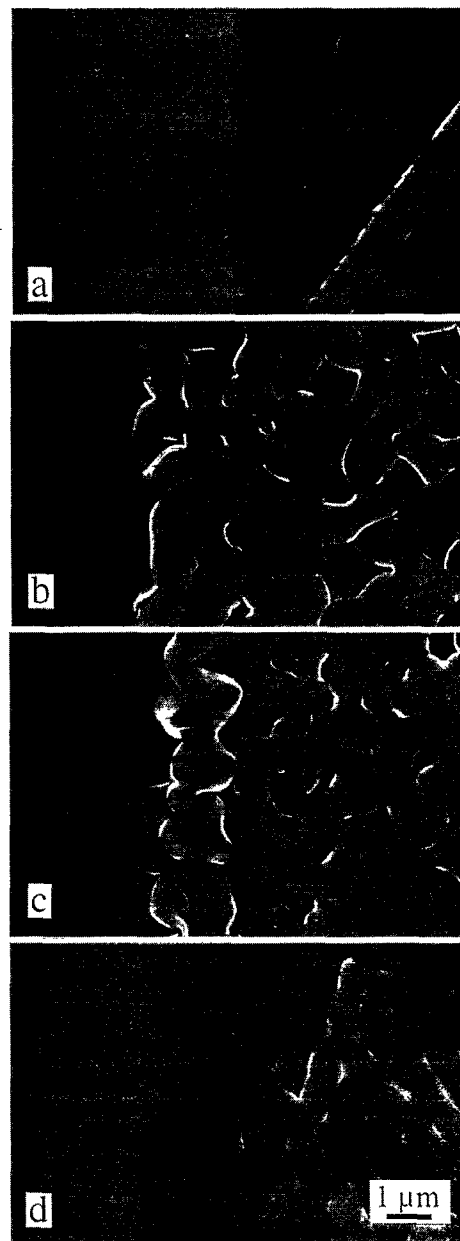


FIG. 3. Scanning microscope micrographs from N-implanted (160 keV) glassy carbon at (a) 5×10^{17} , (b) 1×10^{18} , and (c) 2×10^{18} /cm², and (d) C-implanted (135 keV) glassy carbon at 2×10^{18} /cm².

yield at the end of range is somewhat lower; in addition, the C deficit is shallower and broader. These changes indicate that diffusion of N is occurring away from the implant range both into the sample and toward the surface. A small additional O signal is seen from the surface into the sample for the highest dose.

A simulation of the 5×10^{17} N/cm² backscattering spectrum is shown by the solid line in Fig. 4(a). The simulation models the implanted region using four sublayers each with variable C and N concentrations. The concentrations were varied until an acceptable result was determined visually. From the simulations it is possible to estimate the N concentration. Plots of nitrogen concentration at the implant range and at the surface versus dose are given in Fig. 5. A peak N

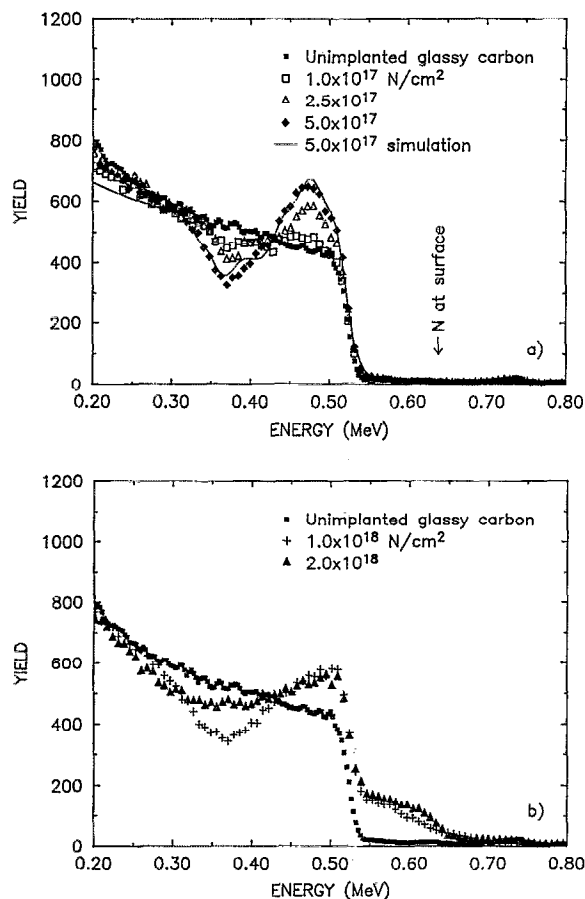


FIG. 4. Rutherford backscattering spectra for N-implanted glassy carbon for doses (a) $\leq 5 \times 10^{17} \text{ N/cm}^2$ and (b) $\geq 1 \times 10^{18} \text{ N/cm}^2$. The data were obtained by backscattering $2 \text{ MeV } ^4\text{He}^+$. Spectra from unimplanted samples are given by the filled squares. The solid line is a simulation of a backscattering spectrum for a sample implanted with $5 \times 10^{17} \text{ N/cm}^2$.

concentration of 30 at. % occurs at the implant range for a dose of $5 \times 10^{17} \text{ N/cm}^2$. Above this dose the end of range concentration falls to near 20 at. % and remains nearly unchanged up to the highest fluence used. The same concentration, 20 at. %, is also seen at the surface for doses between 1 and $2 \times 10^{18} \text{ N/cm}^2$, indicating a rather uniform C:N stoichiometry throughout the implant layer. The RBS simulations also

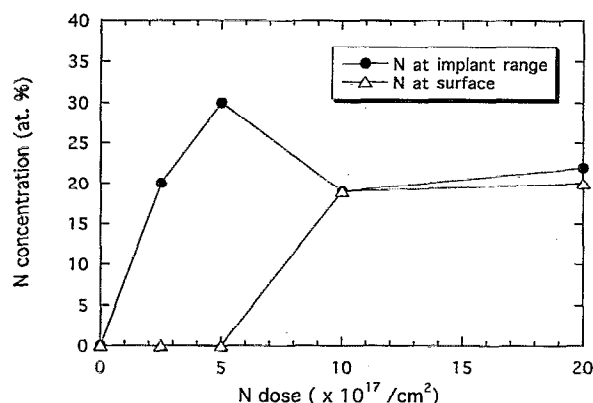


FIG. 5. N concentration vs dose at the implant range and at the surface.

allow an estimate of the total amount of N retained in the sample. The fit in Fig. 3(a) accounts for 95% of the implanted N at a dose of $5 \times 10^{17} \text{ N/cm}^2$. However, up to half of the implanted N is unaccounted for in simulations of the $2 \times 10^{18} \text{ N/cm}^2$ dose.

DISCUSSION

Ion implantation into GC induces a dose-dependent step between the implanted and unimplanted surface regions. Implantation of either N or C leads initially to a compaction of the implanted layer followed by swelling along the normal direction with additional fluence. For doses up to $\sim 3 \times 10^{16} \text{ /cm}^2$, quantitatively similar changes are seen for both C and N, indicating that the step results from damage rather than chemical effects. A similar conclusion has been reported previously.²⁹ Although the lower-energy carbon deposits less energy than N for the same dose and hence would be expected to require roughly 16% more dose for the same compaction,²⁷ this difference is smaller than the uncertainty in the step height measurements. No other techniques have been employed here to confirm that the data of Fig. 1 can be equated to an increased density; however, previously reported results for ion implantation into GC do confirm that compaction is occurring.³⁰ Compaction in GC can easily be understood by considering a model that as implantation amorphizes the graphite ribbon structure of virgin GC, the number and size of the pores are reduced. For N at 160 keV, a maximum step height occurs at a dose of $3 \times 10^{16} \text{ /cm}^2$. Assuming the entire implanted layer ($R_p + \Delta R_p$) has a uniform density and that volume changes are confined to the normal direction, the compaction results in a density $> 2.6 \text{ g/cm}^3$, or greater than 10% denser than sp^2 -bonded graphite but considerably less dense than sp^3 -bonded diamond. It should be mentioned that since the energy deposition in the sample is not uniform with depth, damage-induced density changes are not expected to be uniform.

Similar volume changes accompanying N implantation in GC have been seen previously. In experiments using 50 keV N, densification up to a maximum compaction of 2.6 g/cm^3 were observed.^{31,32} McCulloch and co-workers observed a 2.4 g/cm^3 density following implantation of 50 keV C. The samples were implanted near room temperature in both experiments, in contrast to the present work where the GC was cooled during implantation. Hence, the compaction seen here is not dependent on the sample being implanted below room temperature.

The N dose found here for maximum compaction is $\sim 3 \times 10^{16} \text{ /cm}^2$, or 3 dpa at the peak of the damage deposition distribution. This maximum in density may be responsible for the saturation of other properties observed to reach a limit at approximately this same dpa value,²¹ including an increase in electrical resistance.³³ These changes have been attributed to the complete amorphization of the near surface layer.

At doses greater than that necessary to achieve maximum compaction, expansion of the GC normal to the surface is seen. While this effect is seen for both N and C implantation, it occurs at lower doses for N than for C. This may be partly because of the lower C energy. However, the expansion does not scale according to predictions of energy depo-

sition from TRIM calculations; hence, species-dependent effects are also occurring. For N under the implantation conditions employed here the expansion begins between 3 and $10 \times 10^{16}/\text{cm}^2$ and for C it begins above $1 \times 10^{17}/\text{cm}^2$ and continues up to the highest doses used. From the slope of the initial swelling versus dose region of Fig. 1(b) the volume added per N ion is calculated to be 16 \AA^3 , which is 23% higher than the volume per C atom in unirradiated GC (12.9 \AA^3) and more than twice as large as the volume per atom at the maximum compaction dose of $3 \times 10^{16}/\text{cm}^2$. Assuming a sputter yield of 0.1, there would be some expansion possible from the increased number of atoms in the implanted region. The large expansion is consistent with the introduction of a significant number of point defects in the material. It could also be induced by a phase change driven by chemical effects.

Implantation doses leading to compaction change the color of the GC surface but do not induce any new surface features. In contrast, the SEM micrographs in Fig. 3 clearly show that swelling of the sample is accompanied by a change in surface morphology, at least above a sufficient dose. For N implantation, linear surface features are first seen at a dose of $5 \times 10^{17}/\text{cm}^2$; these evolve into wormlike mounds with additional implantation. The linear appearance of the surface features argues against their being blisters, which for an isotropic material such as amorphous GC would be expected to have a spherical morphology. Similar micron-sized patterns seen before in thin films have been attributed to stress relief,³⁴ and that could well be what is occurring here. Not surprisingly, the appearance of surface features correlates with surface roughening. For C implantation, surface features similar in appearance to those seen for N at 5×10^{17} are also seen, but only at the highest dose studied, 2×10^{18} . Up to this dose no surface roughening is observed. These results indicate that implantation of either N or C into virgin GC initially induces structural changes that are the same; additional implantation into a compacted target leads to species-dependent effects.

Further evidence that phenomena related to a C–N chemistry are occurring can be seen in the RBS results. The surface features and roughening observed using SEM appear at approximately the same N fluence ($5 \times 10^{17}/\text{cm}^2$) at which the N starts to diffuse away from the implant range. A change in the expansion rate is also seen in Fig. 2. Above this dose a rather uniform phase with N comprising ~ 20 at. % is observed from the surface to a depth corresponding to the implant range. Furthermore, this stoichiometry is stable as the N dose is doubled. The additional implanted N is either lost from the surface or diffuses inward. It might be noted that Hoffman *et al.* reported that implantation into GC at a temperature of 400°C yielded a N distribution with a nearly constant concentration of 18 at. % over roughly 150 nm in the sample but with a lower concentration at the surface.¹³ This is close to the uniform N concentration we observe here but for higher N doses and at a much lower implantation temperature. Hoffman *et al.* reported higher N concentrations for their high-dose RT implants.

Based on the evidence presented above, we do not believe that sputtering is the limiting factor controlling the

maximum concentration of N within the implanted layer. For a sputter coefficient of 0.1, under the implantation conditions used in the present experiments the sputter-limited N concentration was calculated by the PROFILE code to be greater than 75 at. %.²⁵ Even for a sputter rate of 1.0, the sputter-limited concentration would be 47 at. %. These values easily exceed the 30 at. % maximum concentration obtained by us in the present work and by others.^{13,21} In addition, the rapid change in the N profile which occurs at a dose between 5×10^{17} and $1 \times 10^{18}/\text{cm}^2$ is not typical of a sputter-limited profile. Rather, we propose that an ion-beam-induced phase change occurs in this dose regime and that concomitant with this phase change N is ejected from the implanted region.

Evidence in support of a phase change was obtained from Raman spectra taken from samples implanted by C (50 keV) to doses of 5×10^{17} and $1 \times 10^{18}/\text{cm}^2$.³⁰ The spectra show evidence for the emergence of polycrystalline graphite within the implanted layer in this dose range. Raman spectra of the N-implanted samples investigated here (not shown) are similar, showing the emergence of polycrystalline graphite peaks for doses between 5×10^{17} and $1 \times 10^{18} \text{ N/cm}^2$. In addition, cross-section transmission electron microscopy investigations of GC implanted with 50 keV C/ cm^2 show clear evidence for the production of oriented graphite crystallites at the end of range and a change in stress from tensile to compressive at a dose of about $5 \times 10^{17} \text{ C/cm}^2$.^{35,36}

These observations lead us to suggest that the N out-diffusion which occurs at a dose between 5×10^{17} and $1 \times 10^{18} \text{ N/cm}^2$ may be the result of an ion-beam-induced reordering of the C into covalently bonded rings. Many compounds are known in which one N substitutes for a C in such rings; for example, pyridine. The relative stability of such compounds may explain the tendency of the layer to saturate to an atomic concentration of about 20 at. % at high N doses.

CONCLUSIONS

Nitrogen and carbon ion implantation into GC causes significant changes in the near-surface morphology. Initially, compaction of the implanted layer from a starting value of 1.5 g/cm^3 to a saturation density of $>2.6 \text{ g/cm}^3$ is observed at nearly the same dose rate for both N and C, indicating the densification is a damage and not a chemical effect. However, at higher doses changes are observed that are species dependent. N implantation beyond the maximum compaction value is accommodated by expansion of the implanted layer and is accompanied by the appearance of linear and then wormlike surface features. It is suggested that this surface morphology results from strain relaxation. While C implantation also leads to expansion and the appearance of linear surface features, the onset of such changes occurs at a significantly higher dose and energy deposition.

For N implantation up to $5 \times 10^{17}/\text{cm}^2$, which corresponds to a maximum local N density of ~ 30 at. %, the N remains at its implant range; however, above this value redistribution of the N is observed and a stable layer with a uniform 20 at. % N stoichiometry is formed from the surface down to the projected range. The appearance of surface features is accompanied by a significant surface roughening. The maximum 30 at. % N concentration achievable under

the implantation conditions used is well below the 57 at. % predicted for β -C₃N₄. The flat N profile is suggestive of a chemical phase. Additional experiments, including Raman and electron spectroscopies, are underway to characterize the chemistry of the implanted N.

ACKNOWLEDGMENTS

The authors would like to acknowledge D. Coffey for assistance in obtaining the SEM micrographs. Research performed at Oak Ridge National Laboratory was supported by the Division of Material Sciences, U. S. Department of Energy, under Contract No. DE-AC05-84OR21400 with Martin Marietta Energy Systems, Inc.

- ¹A. Y. Liu and M. L. Cohen, *Science* **245**, 841 (1989).
- ²K. J. Boyd, D. Marton, S. S. Todorov, A. H. Al-Bayati, J. Kulik, J. W. Rabalais, and R. A. Zuhr (to be published).
- ³D. Marton, A. H. Al-Bayati, S. S. Todorov, K. J. Boyd, and J. W. Rabalais, *Nucl. Instrum. Methods B* **90**, 277 (1994).
- ⁴H. W. Song, F. Z. Cui, W. Z. Li, and H. D. Li, *J. Phys. Condens. Matter* **6**, 6125 (1994).
- ⁵J. F. D. Chubachi, T. Sakai, T. Yamamoto, K. Ogata, A. Ebe, and F. Fujimoto, *Nucl. Instrum. Methods B* **80/81**, 463 (1993).
- ⁶F. Fujimoto and K. Ogata, *Jpn. J. Appl. Phys.* **32**, L420 (1993).
- ⁷C. Niu, Y. Z. Liu, and C. M. Lieber, *Science* **261**, 334 (1993).
- ⁸K. M. Yu, M. L. Cohen, B. E. Haller, W. L. Hansen, A. Y. Liu, and I. C. Wu, *Phys. Rev. B* **49**, 5034 (1994).
- ⁹I. Gouzman, R. Brener, and A. Hoffman, *Thin Solid Films* **253**, 90 (1994).
- ¹⁰A. Hoffman, R. Brener, I. Gouzman, C. Cytermann, H. Geller, L. Levin, and M. Kenny, *Diamond and Related Material* (to be published).
- ¹¹A. Hoffman, I. Gouzman, and R. Brener, *Appl. Phys. Lett.* **64**, 847 (1994).
- ¹²A. Hoffman, C. Cytermann, R. Brener, M. J. Kenny, L. S. Wielunski, and R. A. Clissold, *Nucl. Instrum. Methods B* (to be published).
- ¹³A. Hoffman, H. Geller, I. Gouzman, C. Cytermann, R. Brener, and M. Kenny, *Surf. Coat. Technol.* **68/69**, 616 (1994).
- ¹⁴D. G. McCulloch, Ph.D. thesis, Royal Melbourne Institute of Technology, 1994.
- ¹⁵A. Boussetta, M. Lu, A. Bensaoula, and A. Schultz, *Appl. Phys. Lett.* **65**, 696 (1994).
- ¹⁶H. X. Han and B. J. Feldman, *Solid State Commun.* **65**, 921 (1988).
- ¹⁷L. A. Bursill, J. Peng, V. N. Gurarie, A. V. Orlov, and S. Prawer, *J. Mater. Res.* (to be published).
- ¹⁸T. Sekine, H. Kanda, Y. Bando, M. Yokoyama, and K. Hojou, *J. Mater. Sci. Lett.* **9**, 1376 (1990).
- ¹⁹L. Maya, D. R. Cole, and E. W. Hagamon, *J. Am. Ceram. Soc.* **74**, 1686 (1991).
- ²⁰M. R. Wixom, *J. Am. Ceram. Soc.* **73**, 1973 (1990).
- ²¹M. Iwaki, K. Takahashi, and A. Sekiguchi, *J. Mater. Res.* **5**, 2562 (1990).
- ²²D. G. McCulloch, S. Prawer, and A. Hoffman, *Phys. Rev. B* **50**, 5094 (1994).
- ²³D. G. McCulloch and S. Prawer, *J. Appl. Phys.* (to be published).
- ²⁴Atomergic Chemetals Corporation, New York.
- ²⁵S. N. Bunker and A. J. Armini, *Nucl. Instrum. Methods B* **39**, 7 (1989).
- ²⁶Dektak IIA, Sloan Technology Corp., Santa Barbara, CA.
- ²⁷J. P. Biersack and L. G. Haggmark, *Nucl. Instrum. Methods* **174**, 257 (1980).
- ²⁸W. Eckstein, C. Garcia-Rosales, J. Roth, and W. Ottenberger, Max-Planck-Institut für Plasmaphysik, Report IPP 9/82, 1993.
- ²⁹S. Prawer, F. Ninio, and I. Blanchonette, *J. Appl. Phys.* **68**, 2361 (1990).
- ³⁰D. McCulloch, A. Hoffman, and S. Prawer, *J. Appl. Phys.* **74**, 135 (1993).
- ³¹M. Farrelly and J. T. A. Pollock, *Mater. Forum* **10**, 198 (1987).
- ³²J. T. A. Pollock, R. A. Clissold, and M. Farrelly, *Mater. Res. Soc. Proc.* **93**, 317 (1987).
- ³³D. McCulloch and S. Prawer, *Mater. Res. Soc. Proc.* **187**, 825 (1989).
- ³⁴D. Nir, *Thin Solid Films* **112**, 41 (1984).
- ³⁵D. G. McCulloch, D. R. McKenzie, and S. Prawer, *Philos. Mag.* (to be published).
- ³⁶D. G. McCulloch, N. A. Marks, D. R. McKenzie, and S. Prawer, *Nucl. Instrum. Methods Phys. B* (to be published).